
Article:
Schworer, David, Walkden, Nicholas Ross, Leggate, Huw et al. (Accepted: 2017) Influence of plasma background including neutrals on scrape-off layer filaments using 3D simulations. Nuclear Materials and Energy. ISSN: 2352-1791 (In Press)

https://doi.org/10.1016/j.nme.2017.02.016

Influence of plasma background including neutrals on scrape-off layer filaments using 3D simulations

D. Schwörer[a,b], N. R. Walkden[b], H. Leggate[a], B. D. Dudson[c], F. Militello[b], T. Downes[a], M. M. Turner[a]

[a] *Dublin City University, Dublin 9, Ireland*
[b] *CCFE, Culham Science Centre, Abingdon, Oxfordshire, OX14 3DB, UK*
[c] *University of York, York, Yorkshire, YO10 5DD, UK*

david.schworer2@mail.dcu.ie

1 Abstract

This paper investigates the effect of the plasma background, including neutrals in a self-consistent way, on filaments in the scrape-off layer (SOL) of fusion devices. A strong dependency of filament motion on plasma background density and temperature is observed. The radial filament motion shows an increase in velocity with decreasing background plasma density and increasing background temperature. In the simulations presented here, three neutral-filament interaction models have been compared, one with a static neutral background, one with no interaction between filaments and neutrals, and one co-evolving the neutrals self consistently with the filaments. With the background conditions employed here, which do not show detachment, there are no significant effects of neutrals on filaments, as by the time the filament reaches maximum velocity, the neutral density has not changed significantly.

2 Introduction

Filaments are field-aligned pressure perturbations, observed in most magnetized plasmas [1]. They are intermittent, coherent objects, having a much smaller cross-section perpendicular to the magnetic field than parallel. In tokamaks they can carry a significant amount of heat and particles to the first wall materials, causing e.g. sputtering and thereby diluting the plasma. Further it can cause dust production as well as increase tritium retention, both concerns for ITER [2]. It is therefore of interest to understand these filaments with a view to predicting and controlling them in future devices.

The first simulations of filaments were done in two dimensions [3, 4, 5]. Towards more realistic simulation, three dimensional simulation were studied [6, 7, 8, 9]. At the same time the complexity of the simulation is increased, yielding more realistic simulation [10, 11]. A more detailed review of filament dynamics is given by [1].

In the divertor of future fusion devices the density will increase compared to present-day machines, causing the interaction with neutrals to become even more critical to

machine operation [12]. High neutral densities are expected in the scrape-off layer (SOL), especially in the divertor, making it important to understand in what way neutral interactions can affect filament dynamics.

The interaction between plasma turbulence and neutrals has been recently studied [13, 14, 15]. These studies show the importance of including neutrals in turbulent simulation. They do not address the influence of neutrals on single turbulent structures, as is done in this study. A detailed study of the influence of filaments on neutrals has been conducted [16]. There has been however no study of the influence of neutrals on filaments.

It is assumed that background plasma and neutral profiles can affect filament dynamics, due to non-linearities in the equations [1]. This paper studies the dynamics of filaments in the presence of neutrals. Three neutral-filament interaction models are compared, showing a high level of agreement. The neutrals model varies in the interaction with the filament, ranging from no interaction with the filament to full interaction. Section 3 introduces the model and the setup of the simulations, followed by an introduction of the plasma and neutral backgrounds in section 4. The evolution of the filaments is discussed in section 5, before a short summary is given in section 6.

3 Modelling setup

The model is based on the STORM3D module [8, 9, 11], using BOUT++ [17, 18]. The geometry used is a simplified straight field line SOL geometry. The radial direction is denoted by x. The parallel direction, along the magnetic field is denoted by z, while y is the bi-orthogonal direction. This means y and x span the drift plane. The background features only gradients in parallel direction, but none in radial direction. At $z = \pm L_z = \pm L_\parallel$ is the target. The whole domain is symmetric in z, and only one half is simulated, at $z = 0$ is the symmetry plane. The model includes hot electrons, but cold ions are assumed. Furthermore drift-ordering, following Simakov and Catto [19, 20], is applied.

The neutrals are assumed to be cold, therefore pressure-less, and additionally purely diffusive. As the potential dipole of the filaments forms faster than the neutrals evolve, it is expected that, despite being strongly simplified, the neutral model can capture the relevant physics. Being only the first step in including neutrals, comparison with full kinetic simulations of the neutrals are planned for verification, but this is out of the scope of this paper.

This simple neutral model allows to only evolve the neutral density n_n:

$$\frac{\partial n_n}{\partial t} = \nabla(D_n \nabla n_n) - \Gamma^{\text{ion}} + \Gamma^{\text{rec}} + S_R \tag{1}$$

with ionization rate Γ^{ion}, recombination rate Γ^{rec} and S_R the source due to recycling. In addition the charge exchange rate Γ^{CX} is needed to calculate the effect of the neutrals on the plasma fluid. D_n is the neutral diffusion, given by

$$D_n = \frac{v_{th}^2}{v_{th}\sigma n_n + \Gamma^{\text{CX}} + \Gamma^{\text{ion}}} \tag{2}$$

with v_{th} the thermal speed of deuterium at 300 K and the neutral-neutral cross section $\sigma = \pi(52.9\,\mathrm{pm})^2$. The recycling is proportional to the particle flux at the target $f_T = nU|_{\mathrm{target}}$, the recycling coefficient $f_R = 0.9$ and depending on an exponential recycling falloff length $L_R \approx 18\,\mathrm{cm}$:

$$S_R = \frac{f_R}{L_R} f_T \exp(-z/L_R) \tag{3}$$

A limitation of this recycling model is that recycled particles are redistributed only along magnetic field lines. In the used simple geometry and also allowing diffusion, this is still a reasonable choice. The recycling happens at the wall, but as the diffusion constant is very small for high neutral densities, a non-local model is chosen to compensate for the lack of neutral pressure. Further this is similar to the previously used recycling models in STORM [8, 9, 11].

The full-fluid equations, not differentiating between perturbation and background, for the plasma density n, vorticity ω (arising from current continuity), ion and electron parallel velocity U and V respectively and the electron temperature T are:

$$\frac{\partial n}{\partial t} = \frac{\nabla\phi \times b}{B} \cdot \nabla n - \nabla_\parallel (Vn) + \mu_n \triangle n - gn\frac{\partial \phi}{\partial y} + g\frac{\partial nT}{\partial y} + \Gamma^{\mathrm{ion}} - \Gamma^{\mathrm{rec}} \tag{4}$$

$$\begin{aligned}\frac{\partial w}{\partial t} = {} & \frac{\nabla\phi \times b}{B} \cdot \nabla w - U\nabla_\parallel w + \nabla_\parallel (U - V) + \frac{U - V}{n}\nabla_\parallel n + \mu_w \triangle w \\ & + \nabla_\perp \mu_w \cdot \nabla_\perp w + \frac{g}{n}\frac{\partial nT}{\partial y} + \triangle_\perp \phi(\Gamma^{\mathrm{CX}} + \Gamma^{\mathrm{ion}})\end{aligned} \tag{5}$$

$$\begin{aligned}\frac{\partial U}{\partial t} = {} & \frac{\nabla\phi \times b}{B} \cdot \nabla U - U\nabla_\parallel U - \nabla_\parallel \phi - \eta_\parallel n(U - V) \\ & + 0.71\nabla_\parallel T - \frac{U}{n}\Gamma^{\mathrm{ion}} - \frac{U}{n}\Gamma^{\mathrm{CX}}\end{aligned} \tag{6}$$

$$\begin{aligned}\frac{\partial V}{\partial t} = {} & \frac{\nabla\phi \times b}{B} \cdot \nabla V - V\nabla_\parallel V + \mu\nabla_\parallel \phi - \frac{\mu}{n}\nabla_\parallel nT \\ & + n\mu\eta_\parallel (U - V) - 0.71\mu\nabla_\parallel T - \frac{V}{n}\Gamma^{\mathrm{ion}}\end{aligned} \tag{7}$$

$$\begin{aligned}\frac{\partial T}{\partial t} = {} & \frac{\nabla\phi \times b}{B} \cdot \nabla T - V\nabla_\parallel T + \frac{2}{3}\left(\frac{-1}{n}\nabla_\parallel q_\parallel + 0.71(U - V)\nabla_\parallel T - T\nabla_\parallel V\right. \\ & \left. + \frac{\kappa_\perp}{n} \triangle_\perp T - \eta_\parallel n(U - V)^2\right) - \frac{2}{3}gT\frac{\partial \phi}{\partial y} - \frac{2}{3}g\frac{T^2}{n}\frac{\partial n}{\partial y} - \frac{7}{3}gT\frac{\partial T}{\partial y} \\ & - \frac{2}{3}gV^2\frac{1}{\mu n}\frac{\partial nT}{\partial y} - \frac{T}{n}\Gamma^{\mathrm{ion}}\end{aligned} \tag{8}$$

with $\mu = m_i/m_e$ the ion-electron mass ratio, μ_α the respectively diffusion constants, $q_\parallel$ the parallel heat conduction and $\eta_\parallel$ the ion-electron collisionality. Note that all collisionalities, including diffusion constants, are calculated self consistently [11]. The constant g is related to the radius of curvature R_c as $g = \frac{2}{R_c}$. As a slab geometry is used, these terms need to be introduced artificially in the equations.

The boundary condition are Neumann in x (corresponding to radial direction) for all variables, except ϕ and ω, which are kept at there background values, and periodic in y

direction for all quantities. At the symmetry plane (upper z) the boundary conditions are Neumann, for all but the flow velocities, which are set to zero. At the target (lower z) the ions need to be at the speed of sound $U = \sqrt{T}$, and the electron velocity is

$$V = \sqrt{T} \exp(-V_f - \frac{\phi}{T}) \tag{9}$$

with the floating potential V_f and the electrostatic potential ϕ. The neutrals have Neumann boundary conditions at the target.

The filament simulations are carried out on a domain with x (corresponding to radial direction) and y dimensions 20 cm and 128 grid points, resulting in a grid spacing of 1.5625 mm. In the parallel direction (z) 64 grid points are used and the parallel length is 10 m, giving a grid spacing of 15.625 cm. 10 m is a typical connection-length for MAST double null plasma.

In order to run the filament simulation, a background is needed. This is achieved by running a one-dimensional simulation to steady state. A detailed description is given by Walkden in the appendix of ref. [11]. The aim is to study the role played by neutrals on filament dynamics by comparing the evolution of filaments, given a static neutrals background, and co-evolving the neutrals self consistently with the other plasma quantities.

The filaments were seeded as temperature and density perturbation, with amplitude δ_T and δ_n on top of a background. The perpendicular size $\delta_\perp$, defined as the Gaussian width, of each filament was set to $\delta_\perp = 2\,\mathrm{cm}$, as the filaments observed in MAST are about this size [21, 22]. The plasma parameters where chosen to be relevant for MAST, however due to the simplified geometry no direct comparison with MAST filaments is possible. The scaling parameter δ^* [3, 23] for the simulation is in the range of 1.3 cm to 2.3 cm. As the perpendicular size of the filaments is in the range of δ^*, the observed findings are not limited to MAST [11]. The initial perturbation is set to $\delta_T = 40\,\mathrm{eV}$ and $\delta_n = 8 \times 10^{18}\,\mathrm{m}^{-3}$ above the background. In a second run, the initial perturbation are set to the mid-plane value of the background values. In this case the initial temperature perturbations varied between 12 eV and 48 eV and density perturbations are in the range of 8 to $24 \times 10^{18}\,\mathrm{m}^{-3}$. The second case keeps the ratios $\frac{\delta n + n_0}{n_0} = 2$ and $\frac{\delta T + T_0}{T_0} = 2$ constant. This allows to differentiate the effects due to changing drive of the filament's motion, and changing interaction with the background, including neutrals.

After seeding the filaments, the fields where evolved using the equations provided in sec. 3. The neutrals have been included in different ways in the filament simulations. In one run the source/sinks terms related to the neutrals $\Gamma^{\mathrm{CX}}, \Gamma^{\mathrm{ion}}$ and Γ^{rec} are given by the steady state values. This is the case of no direct interaction of the filaments with the neutrals. In a second case, the neutral density is given by the steady state values, but ionization, etc. are computed. In a third case the neutrals where co-evolved with the filaments.

The velocity of the filaments is computed by tracking the centre of each of density, temperature or pressure perturbation.

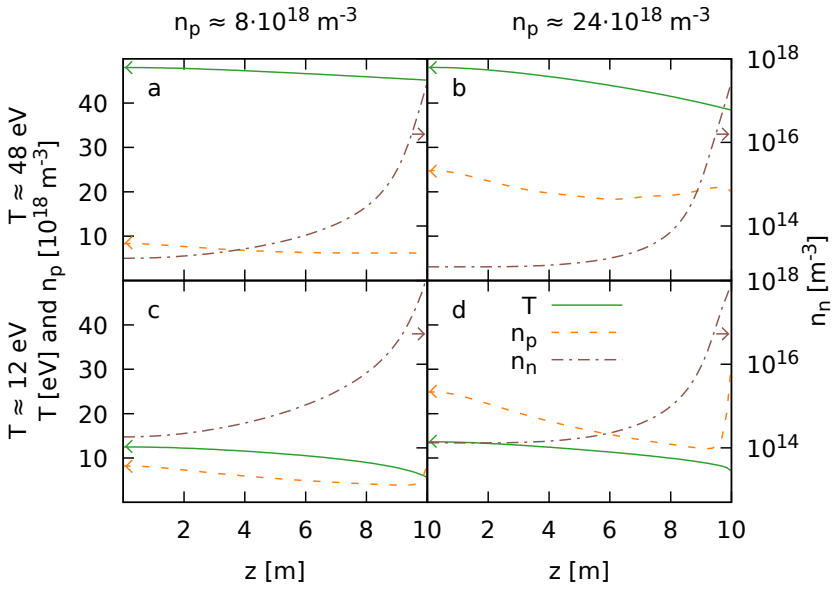

Figure 1: Background plasma profiles, run to steady-state for a given influx of energy and particles. The sheath is at the right hand side at $L = 10\,\mathrm{m}$. The mid-plane is at the left side, and is used as symmetry plane. The profiles a and b have an electron background temperature of $\sim 48\,\mathrm{eV}$ at the mid-plane, while c and d have a background temperature of $\sim 12\,\mathrm{eV}$. The background density for a and c is $n_p \approx 8 \times 10^{18}\,\mathrm{m}^{-3}$, for b and d $n_p \approx 24 \times 10^{18}\,\mathrm{m}^{-3}$ at the mid-plane. Plasma density and temperature is plotted to the linear scale on the left hand side. The neutral density n_n is plotted to the log scale on the right hand side.

4 Background profiles

The different particle and energy influx in the steady state simulations allowed for different SOL regimes to be investigated [24]. Fig. 1 shows temperature and density of the electrons, as well as neutral densities. The low temperature simulations are in the high recycling regime, as the temperature drops to around half its mid-plain value. The high temperature ones are in the low recycling regime [24]. The maximum parallel temperature gradients are between $0.38\,\mathrm{eV/m}$ and $12.1\,\mathrm{eV/m}$. The maximum parallel plasma density gradients are between 5 and $71 \times 10^{18}\,\mathrm{m}^{-4}$ and for the neutrals between 3 and $46{\times}10^{18}\,\mathrm{m}^{-4}$

5 Filament evolution

An example of the evolution of a filament is shown in fig. 2. The figure shows the time evolution of the density. It can be seen that the filament is not symmetric in y-direction. Additional to the radial motion, a motion in y direction is observed. This

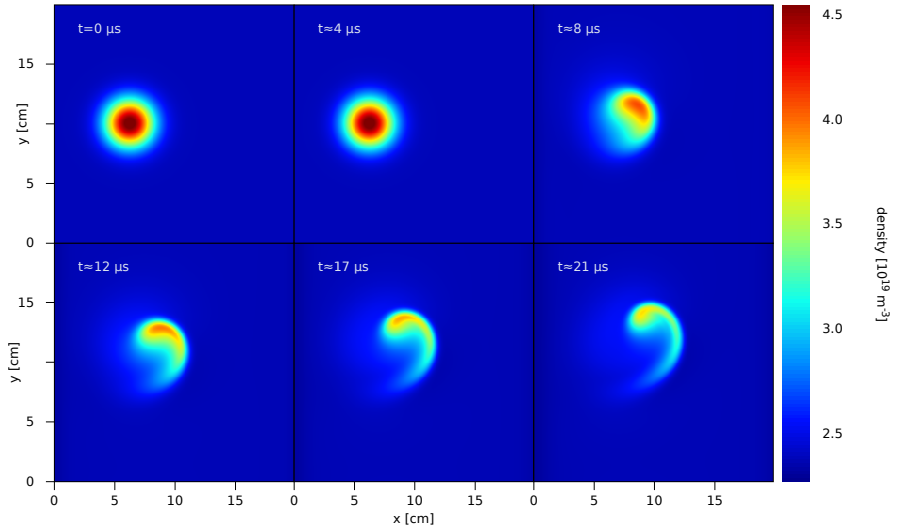

Figure 2: Snapshots of the time evolution of the density of the filament in the perpendicular direction, close to the mid-plane. The symmetry plane background density was $n_0 \approx 24 \times 10^{18}\,\mathrm{m}^{-3}$ and $T_0 \approx 48\,\mathrm{eV}$. The initially seeded perturbation, shown in a, is equal to the background values. b-f are each separated by $\sim 4\,\mu\mathrm{s}$.

behaviour has been observed and discussed [11, 25].

The measured radial velocities for the blobs of initial amplitude $\delta T = 40\,\mathrm{eV}$ and $\delta n = 8 \times 10^{18}\,\mathrm{m}^{-3}$ above the background are shown in fig. 3. It can be seen that the maximum velocities of the filaments, derived from the centre of density, temperature or pressure, differ. The variation is higher for filaments with larger amplitude and higher background temperature. The density derived velocities are higher than the temperature derived velocities. The pressure derived velocities, as pressure being the product of density and temperature, lie between those. Due to the seeding process the filaments start with no initial velocity. Therefore the initial velocities are ignored, and only the maximum velocities are taken into account for the further discussion.

As can be seen in fig. 4 evolving the neutrals background changes the filament dynamic slightly. However any changes are small and do not affect the peak velocity. Using the steady state rates, instead of calculating the rates based on the filaments density, does not significantly affect the filaments motion. This suggests that the neutrals do not have a significant, direct effect on the filaments, however the neutrals influence the background profiles, which changes the filament dynamics. These simulation do not feature detachment which would increase the neutral densities where the direct influence of neutrals on filaments might become important. Easy et al. shows that the temperature needs to drop below 1 eV at the target for the neutrals to have a significant effect on the parallel resistivity, to influences the filament dynamic [9]. Further, none of the models is fully able to capture the physics of neutrals correctly, which would require a kinetic approach, e.g. using EIRENE [26], but this is computationally challenging. To compare with experiments, a realistic geometry would be

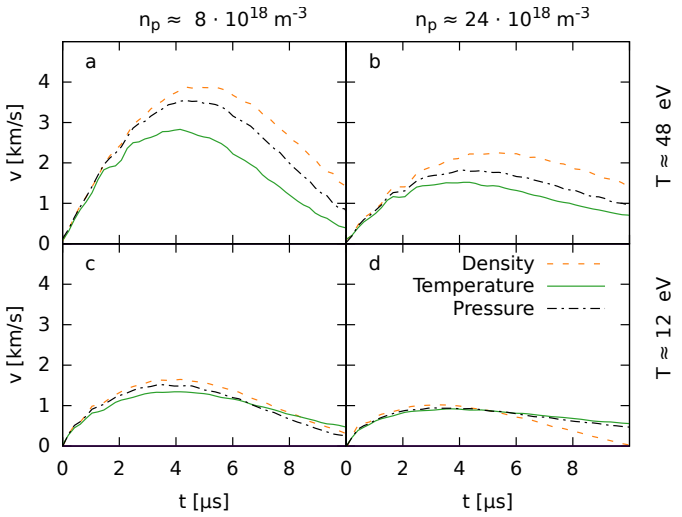

Figure 3: Time evolution of filament velocity, derived from the centre of density (orange dashed), temperature (green line) and pressure (black dot-dashed). See fig. 1 for label a-d description. Note that the filaments initially accelerate, as the potential needs to evolve. This is due to the seeding process. The velocities near the symmetry plane, i.e. $z \approx 0$.

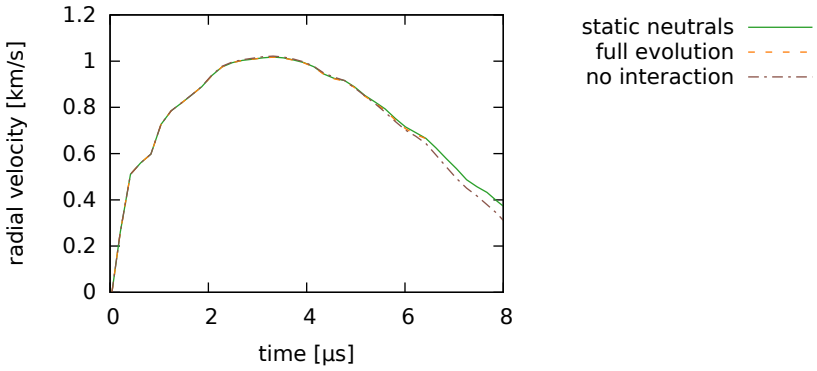

Figure 4: Comparison of full co-evolution of neutrals with filaments, fixed neutral background and equilibrium neutral rates i.e. no interaction of the filaments with the neutrals. This is for the case of $T_0 \approx 12\,\mathrm{eV}$ and $n_0 \approx 8 \times 10^{18}\,\mathrm{m}^{-3}$, the case with the strongest difference between the three models.

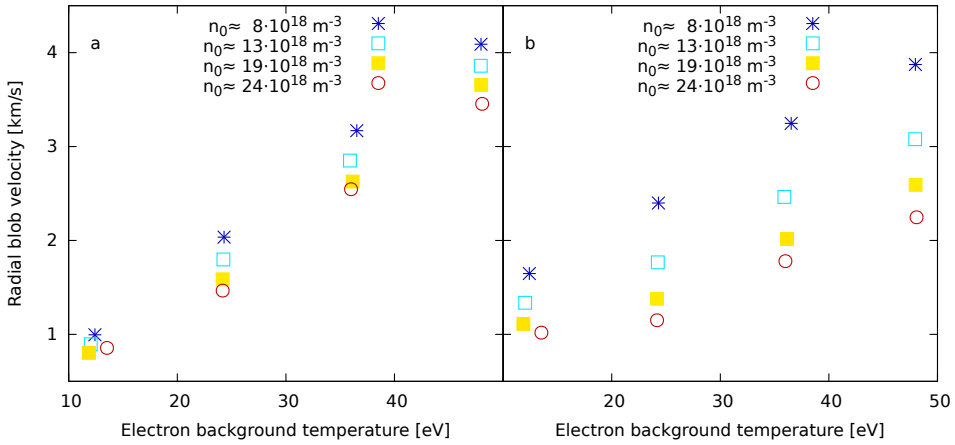

Figure 5: Maxima of radial filament velocities in km/s in dependency of background density and temperature. The filaments in a have an initial amplitude equal to the respective background, i.e. $(\delta n + n_0)/n_0 = 2$. The filaments shown in b have all an initial amplitude of $\delta_T = 40\,\mathrm{eV}$ and $\delta_n = 8 \times 10^{18}\,\mathrm{m}^{-3}$.

needed.

Figure 4 compares the three neutrals models. It shows a barely noticeably difference only for times after the peak velocity is reached. This may be caused by the fact that the neutral density near the mid-plane do not change significantly in the first µs of the filament simulation. This is partly due to the fast diffusion, also limiting the computational time step. This means that, although neutrals get ionized faster in the filament than in the previously run background simulation, the depletion is only notable for times after the filament reaches maximum velocity, as neutrals from outside the filament refuel the neutrals in the filament.

Near the target, a second effect comes into play. The filament, being denser than the background, increases recycling of the neutrals. Furthermore the hotter, denser filament ionizes more neutrals. These two effects are therefore compensating each other, allowing the static neutrals to have a good agreement with the co-evolving case.

Fig. 5 shows the peak values of the radial velocities as a function of both the background density and temperature. For the series with filament amplitude relative to the background, shown in a, the filaments move faster with increasing temperature. For a given temperature, both $\delta n/n$ as well as $\delta p/n$ are constant. The radial velocity decreases with increasing density.

The scaling for the filament motion in radial direction can be derived as $v \propto c_s \delta_\perp^{1/2} \propto T^{1/2}\delta_\perp^{1/2}$ in the inertial limited regime, and as $v \propto c_s T \delta_\perp^{-2} \propto T^{3/2}\delta_\perp^{-2}$ in the sheath limited regime [11]. Note that no dependency on the background density is expected if the perturbation δ_n is scaled with the background value n_0. Also the scaling with the temperature should be T^α with $\frac{1}{2} \leq \alpha \leq \frac{3}{2}$. In terms of the temperature dependency, the simulations lie within the range of the scaling. The density dependency in a

can however not be explained. With the exception of $T \approx 12\,\mathrm{eV}$ cases, the filament velocities in b, i.e. for constant filament amplitude, increase as well with background temperature. A monotone decrease of radial velocity with increase in background density is observed, again with the exception for low temperatures. The dependency on the background density is higher in b, as the drive $\delta p/n$ changes, unlike in a.

The simulations show that the velocity is not only determined by $\delta p/n$. Otherwise, all points at the same temperature in part a should collapse on one point in fig. 5. The 2D scaling law does not include density dependence of the dependent variables, therefore the deviation is probably not only due to neutrals. See e.g. ref. [9] for a discussion of the importance of parallel resistivity.

6 Summary

This paper presents the influence of the plasma background, including neutrals, on filaments. The plasma background has an impact on filament motion. For filaments, representative of those found in MAST, the radial motions shows a decrease with increasing background density n_0 and an increase with increasing background temperature T_0. The density dependency cannot be accounted for by ether sheath limited nor inertial limited theory and may indicate the importance of plasma resistivity. In the filament simulation, three neutral-filament interaction models have been compared, one keeping the background ionisation-, recombination- and charge-exchange-rate, one keeping the neutrals static, and a third one co-evolving the neutrals with the filament. This first corresponds to no interaction between the filament and neutrals, while the third features full interaction. The static neutral-filament interaction model showed, especially for times shorter than $\sim 6\,\mu\mathrm{s}$, a good agreement with the self consistent evolution of the neutrals. This is in part due to, on the time-scale upon which the filament reaches its maximum velocity, minimal change occurs in the neutral density. By the time the neutral density reaches a minimum the filament has moved significantly from its starting position.

The neutral model used is a strongly simplified. In order to verify that it can capture the relevant physic, a comparison with a full kinetic neutral model would be beneficial. One option would be a coupled version of BOUT++ with EIRENE [26]. This would allow to use the EIRENE neutral solver framework to model the neutrals in a realistic way. Including background gradients in radial direction, as well as switching to more realistic geometries, would allow better comparison with experiments.

7 Acknowledgement

This work has been carried out within the framework of the EUROfusion Consortium and has received funding from the Euratom research and training programme 2014-2018 under grant agreement No 633053 and from the RCUK Energy Programme [grant number EP/I501045]. To obtain further information on the data and models underlying this paper please contact PublicationsManager@ccfe.ac.uk*. The views and

opinions expressed herein do not necessarily reflect those of the European Commission. Simulations in this paper made use of the ARCHER UK National Supercomputing service (www.archer.ac.uk) under the Plasma HEC Consortium EPSRC grant number EP/L000237/1 and of the Irish Centre for High-End Computing (ICHEC) computational facilities.

References

[1] D. D'Ippolito, J. Myra, and S. Zweben, "Convective transport by intermittent blob-filaments: Comparison of theory and experiment," *Physics of Plasmas (1994-present)*, vol. 18, no. 6, p. 060501, 2011.

[2] J. Roth, E. Tsitrone, A. Loarte, T. Loarer, G. Counsell, R. Neu, V. Philipps, S. Brezinsek, M. Lehnen, P. Coad, C. Grisolia, K. Schmid, K. Krieger, A. Kallenbach, B. Lipschultz, R. Doerner, R. Causey, V. Alimov, W. Shu, O. Ogorodnikova, A. Kirschner, G. Federici, and A. Kukushkin, "Recent analysis of key plasma wall interactions issues for ITER," *Journal of Nuclear Materials*, vol. 390–391, pp. 1 – 9, 2009.

[3] G. Q. Yu and S. I. Krasheninnikov, "Dynamics of blobs in scrape-off-layer/shadow regions of tokamaks and linear devices," *Physics of Plasmas*, vol. 10, no. 11, pp. 4413–4418, 2003.

[4] G. Yu, S. Krasheninnikov, and P. Guzdar, "Two-dimensional modelling of blob dynamics in tokamak edge plasmas," *Physics of Plasmas (1994-present)*, vol. 13, no. 4, p. 042508, 2006.

[5] O. Garcia, N. Bian, and W. Fundamenski, "Radial interchange motions of plasma filaments," *Physics of Plasmas (1994-present)*, vol. 13, no. 8, p. 082309, 2006.

[6] D. Jovanović, P. Shukla, and F. Pegoraro, "Effects of the parallel electron dynamics and finite ion temperature on the plasma blob propagation in the scrape-off layer," *Physics of Plasmas (1994-present)*, vol. 15, no. 11, p. 112305, 2008.

[7] J. R. Angus, M. V. Umansky, and S. I. Krasheninnikov, "Effect of drift waves on plasma blob dynamics," *Phys. Rev. Lett.*, vol. 108, p. 215002, May 2012.

[8] L. Easy, F. Militello, J. Omotani, B. Dudson, E. Havlíčková, P. Tamain, V. Naulin, and A. H. Nielsen, "Three dimensional simulations of plasma filaments in the scrape off layer: A comparison with models of reduced dimensionality," *Physics of Plasmas*, vol. 21, no. 12, 2014.

[9] L. Easy, F. Militello, J. Omotani, N. Walkden, and B. Dudson, "Investigation of the effect of resistivity on scrape off layer filaments using three-dimensional simulations," *Physics of Plasmas (1994-present)*, vol. 23, no. 1, p. 012512, 2016.

[10] N. R. Walkden, B. D. Dudson, and G. Fishpool, "Characterization of 3d filament dynamics in a MAST SOL flux tube geometry," *Plasma Physics and Controlled Fusion*, vol. 55, no. 10, p. 105005, 2013.

[11] N. R. Walkden, L. Easy, F. Militello, and J. T. Omotani, "Dynamics of 3d isolated thermal filaments," *Plasma Physics and Controlled Fusion*, vol. 58, no. 11, p. 115010, 2016.

[12] B. LaBombard, M. Umansky, R. Boivin, J. Goetz, J. Hughes, B. Lipschultz, D. Mossessian, C. Pitcher, J. Terry, and A. Group, "Cross-field plasma transport and main-chamber recycling in diverted plasmas on alcator c-mod," *Nuclear Fusion*, vol. 40, no. 12, p. 2041, 2000.

[13] J. Leddy, H. V. Willett, and B. D. Dudson, "Simulation of the interaction between plasma turbulence and neutrals in linear devices," *Nuclear Materials and Energy*, October 2016. This is an author-produced version of the published paper. Uploaded in accordance with the publisher?s self-archiving policy. Further copying may not be permitted; contact the publisher for details. (no embargo).

[14] N. Bisai and P. Kaw, "Role of neutral gas in scrape-off layer of tokamak plasma in the presence of finite electron temperature and its gradient," *Physics of Plasmas (1994-present)*, vol. 23, no. 9, p. 092509, 2016.

[15] C. Wersal and P. Ricci, "A first-principles self-consistent model of plasma turbulence and kinetic neutral dynamics in the tokamak scrape-off layer," *Nuclear Fusion*, vol. 55, no. 12, p. 123014, 2015.

[16] A. S. Thrysøe, L. E. H. Tophøj, V. Naulin, J. J. Rasmussen, J. Madsen, and A. H. Nielsen, "The influence of blobs on neutral particles in the scrape-off layer," *Plasma Physics and Controlled Fusion*, vol. 58, no. 4, p. 044010, 2016.

[17] B. Dudson, M. Umansky, X. Xu, P. Snyder, and H. Wilson, "BOUT++: A framework for parallel plasma fluid simulations," *Computer Physics Communications*, vol. 180, no. 9, pp. 1467 – 1480, 2009.

[18] B. D. Dudson, A. Allen, G. Breyiannis, E. Brugger, J. Buchanan, L. Easy, S. Farley, I. Joseph, M. Kim, A. D. McGann, J. T. Omotani, M. V. Umansky, N. R. Walkden, T. Xia, and X. Q. Xu, "BOUT++: Recent and current developments," *Journal of Plasma Physics*, vol. 81, 1 2015.

[19] A. N. Simakov and P. J. Catto, "Drift-ordered fluid equations for field-aligned modes in low-β collisional plasma with equilibrium pressure pedestals," *Physics of Plasmas*, vol. 10, no. 12, pp. 4744–4757, 2003.

[20] A. N. Simakov and P. J. Catto, "Erratum: "drift-ordered fluid equations for field-aligned modes in low-β collisional plasma with equilibrium pressure pedestals" [phys. plasmas 10, 4744 (2003)]," *Physics of Plasmas*, vol. 11, no. 5, pp. 2326–2326, 2004.

[21] B. D. Dudson, N. B. Ayed, A. Kirk, H. R. Wilson, G. Counsell, X. Xu, M. Umansky, P. B. Snyder, B. LLoyd, and the MAST team, "Experiments and simulation of edge turbulence and filaments in MAST," *Plasma Physics and Controlled Fusion*, vol. 50, no. 12, p. 124012, 2008.

[22] A. Kirk, N. B. Ayed, G. Counsell, B. Dudson, T. Eich, A. Herrmann, B. Koch, R. Martin, A. Meakins, S. Saarelma, R. Scannell, S. Tallents, M. Walsh, H. R. Wilson, and the MAST team, "Filament structures at the plasma edge on MAST," *Plasma Physics and Controlled Fusion*, vol. 48, no. 12B, p. B433, 2006.

[23] J. R. Myra, D. A. D'Ippolito, D. P. Stotler, S. J. Zweben, B. P. LeBlanc, J. E. Menard, R. J. Maqueda, and J. Boedo, "Blob birth and transport in the tokamak edge plasma: Analysis of imaging data," *Physics of Plasmas*, vol. 13, no. 9, 2006.

[24] P. C. Stangeby *et al.*, *The plasma boundary of magnetic fusion devices*, vol. 224. Institute of Physics Publishing Bristol, 2000.

[25] J. Myra, D. D'ippolito, S. Krasheninnikov, and G. Yu, "Convective transport in the scrape-off-layer by nonthermalized spinning blobs," *Physics of Plasmas (1994-present)*, vol. 11, no. 9, pp. 4267–4274, 2004.

[26] D. Reiter, M. Baelmans, and P. Börner, "The EIRENE and B2-EIRENE codes," *Fusion Science and Technology*, vol. 47, no. 2, pp. 172–186, 2005.